ORIGINAL RESEARCH

Application of Magnetocardiography to Screen for Inflammatory Cardiomyopathy and Monitor Treatment Response

Debora Brala, MD*; Tharusan Thevathasan ⬦, MD*; Simon Grahl ⬦; Steve Barrow, PhD; Michele Violano, MD; Hendrikje Bergs ⬦; Ainoosh Golpour ⬦; Phillip Suwalski ⬦; Wolfgang Poller ⬦, MD; Carsten Skurk ⬦, MD; Ulf Landmesser, MD; Bettina Heidecker ⬦, MD

BACKGROUND: Inflammatory cardiomyopathy is one of the most common causes of sudden cardiac death in young adults. Diagnosis of inflammatory cardiomyopathy remains challenging, and better monitoring tools are needed. We present magnetocardiography as a method to diagnose myocardial inflammation and monitor treatment response.

METHODS AND RESULTS: A total of 233 patients were enrolled, with a mean age of 45 (±18) years, and 105 (45%) were women. The primary analysis included 209 adult subjects, of whom 66 (32%) were diagnosed with inflammatory cardiomyopathy, 17 (8%) were diagnosed with cardiac amyloidosis, and 35 (17%) were diagnosed with other types of nonischemic cardiomyopathy; 91 (44%) did not have cardiomyopathy. The second analysis included 13 patients with inflammatory cardiomyopathy who underwent immunosuppressive therapy after baseline magnetocardiography measurement. Finally, diagnostic accuracy of magnetocardiography was tested in 3 independent cohorts (total n=23) and 1 patient, who developed vaccine-related myocarditis. First, we identified a magnetocardiography vector to differentiate between patients with cardiomyopathy versus patients without cardiomyopathy (vector of ≥0.051; sensitivity, 0.59; specificity, 0.95; positive predictive value, 93%; and negative predictive value, 64%). All patients with inflammatory cardiomyopathy, including a patient with mRNA vaccine-related myocarditis, had a magnetocardiography vector ≥0.051. Second, we evaluated the ability of the magnetocardiography vector to reflect treatment response. We observed a decrease of the pathologic magnetocardiography vector toward normal in all 13 patients who were clinically improving under immunosuppressive therapy. Magnetocardiography detected treatment response as early as day 7, whereas echocardiographic detection of treatment response occurred after 1 month. The magnetocardiography vector decreased from 0.10 at baseline to 0.07 within 7 days (P=0.010) and to 0.03 within 30 days ($P<0.001$). After 30 days, left ventricular ejection fraction improved from 42.2% at baseline to 53.8% ($P<0.001$).

CONCLUSIONS: Magnetocardiography has the potential to be used for diagnostic screening and to monitor early treatment response. The method is valuable in inflammatory cardiomyopathy, where there is a major unmet need for early diagnosis and monitoring response to immunosuppressive therapy.

Key Words: COVID-19 ■ echocardiography ■ ejection fraction ■ immunosuppressive therapy ■ inflammatory cardiomyopathy ■ magnetocardiography

Inflammatory cardiomyopathy is a common cause of heart failure,[1] which may lead to circulatory collapse, requiring mechanical circulatory support or heart transplant. It is also one of the most common causes of sudden cardiac death in young adults, as it frequently remains undetected.[2,3] Some patients may require

CLINICAL PERSPECTIVE

What Is New?

- We report magnetocardiography as a novel method to screen for inflammatory cardiomyopathy and monitor treatment response to immunosuppression as early as day 7 ($P<0.01$), whereas echocardiographic detection of treatment response occurred after 1 month ($P<0.001$).
- Furthermore, magnetocardiography was able to differentiate between patients with cardiomyopathy versus patients without cardiomyopathy overall (vector of ≥0.051); the sensitivity was 0.59, the specificity was 0.95, the positive predictive value was 93%, and the negative predictive value was 64%.

What Are the Clinical Implications?

- There is a major unmet need for (1) broad diagnostic screening in inflammatory cardiomyopathy to prevent cardiovascular complications, including sudden cardiac death; and (2) monitoring early treatment response to individualize therapy; both areas may be addressed through the application of magnetocardiography in the future.

Nonstandard Abbreviations and Acronyms

EMB	endomyocardial biopsy
FDG-PET-CT	fluorodeoxyglucose–positron emission tomography–computed tomography

immunosuppression in addition to standard heart failure therapy.[2,4–7] In patients in whom inflammation progresses despite those measures, an escalation of immunosuppressive therapy may be warranted.[8] Measuring response to treatment has been a major clinical challenge in these patients, as current state-of-the-art diagnostic methods in inflammatory cardiomyopathy have limitations in detecting early treatment response. Echocardiography provides valuable structural and hemodynamic data of the heart, enabling the identification of indirect signs of inflammation, such as impaired left ventricular function or wall motion abnormalities. Similarly, cardiac magnetic resonance imaging (CMR) provides comprehensive structural and functional data while detecting consequences of inflammation, such as edema and late gadolinium enhancement.[9] Fluorodeoxyglucose–positron emission tomography–computed tomography (FDG-PET-CT) detects the level of activity and the extent of inflammation through measurement of glucose metabolism. However, it cannot be applied frequently because of the associated radiation exposure. Endomyocardial biopsy (EMB) is the gold standard for definitive diagnosis of inflammatory cardiomyopathy and is crucial for initiation of immunosuppressive therapy, as active viral infection must be excluded.[2,3,5,10] However, the risk of potential complications and limited diagnostic yield (diagnostic sensitivity, ≈64%–92% with multiple samples) limit its use for frequent short-term follow-up.[5,11,12]

Given these limitations in detecting early treatment response, optimal immunosuppressive therapy and its surveillance in patients with inflammatory cardiomyopathy remain a major clinical challenge. Consequently, some patients may undergo a trial-and-error treatment approach for several months to years and experience worsening of their clinical condition until the lack of response is detected and immunosuppression adjusted.

To address this issue, we tested the value of magnetocardiography to screen for inflammatory cardiomyopathy and to detect early treatment response during immunosuppressive therapy compared with echocardiography. In addition, we tested the diagnostic accuracy of magnetocardiography in 3 independent cohorts: (1) patients without inflammatory cardiomyopathy receiving immunosuppression; (2) patients with inflammatory cardiomyopathy without immunosuppressive therapy; and (3) patients with post–COVID-19 condition with neither inflammatory cardiomyopathy nor immunosuppressive therapy. Finally, we tested generalizability of magnetocardiography for the detection of inflammatory cardiomyopathy in mRNA vaccine-related myocarditis.

Magnetocardiography is a noninvasive method with the ability to detect the cardiac magnetic field generated by electrical currents of the heart (Figure S1 and S2 and Figure 1).[13–16] Magnetocardiography has the capability to detect the magnetic field of the heart at a high level of precision (10^{-15} to 10^{-11} T).

In a normal heart, the heart's magnetic field defines a fixed orientation and magnitude characterized by a vector. When illustrated in a magnetocardiography display, this vector is typically located in the first quadrant (Figure S3). In case of a pathology of the heart or in cardiomyopathies generally, there are fluctuations in both the magnitude and orientation of the heart's magnetic field, leading to a position of the vector in the second and third quadrant of the display of a magnetocardiograph (Figure S3).[17,18]

The objective of our study was to screen for inflammatory cardiomyopathy and to monitor response to therapy by measuring the heart's magnetic field vector in terms of its magnitude and direction during immunosuppressive therapy (Figure 1).[17–20]

Magnetocardiography offers many practical advantages compared with other diagnostic methods.
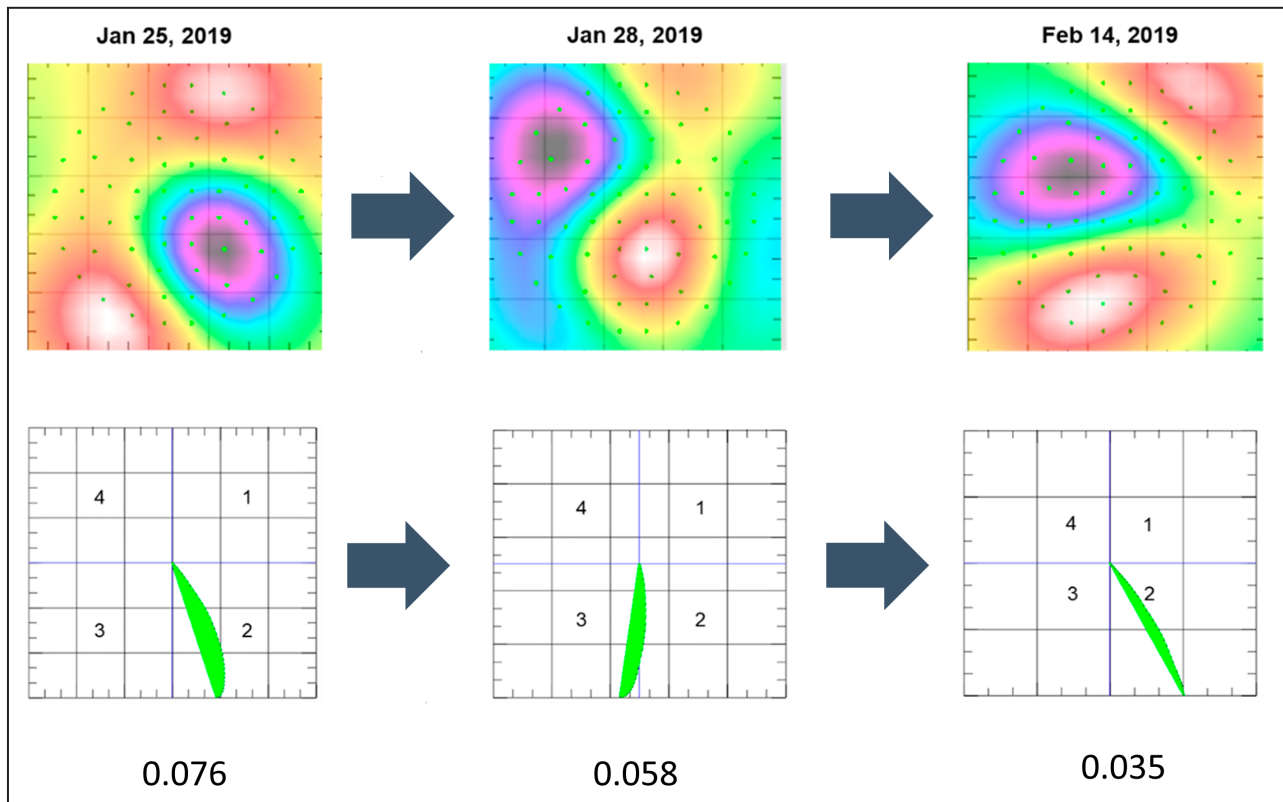
Figure 1. Evolution of the magnetic field during treatment of a subject with inflammatory cardiomyopathy (exemplary).
Magnetocardiography (MCG) measures cardiac magnetic fields tangential to the chest surface by using 64 first-order gradiometers in an area of 162×162 mm with a sensor interval of ≈35 mm. The MCG signals were recorded at a sampling rate of 512 Hz. The inserted sensor array of type II consists of 48 tangential sensors and 16 axial sensors, which can measure magnetic field components along all 3 axes. In comparison, the older sensor type I consists of 64 axial sensors. The main dimensions of the sensor array are shown in Figure 1. The outer sensor circle has a diameter of 246 mm. First-order gradiometer pickup coils are used with a passive magnetically shielding room (MSR) to reduce the external magnetic noise to an acceptable level. To achieve this, 4 layers of mu-metal have been installed in the MSR. *First row*: The graphics show changes in heart polarization during immunosuppressive therapy. MCG measures the heart's magnetic field in 3 axes (x, y, and z). The colors represent the strength of the magnetic field on the sagittal plane (z axis). The sizes and positions of the magnetic fields are reported in millimeters. The negative pole (minimal measured magnetic field strength) is colored in black, and the positive poles (maximal measured magnetic field strength) is colored in white. All other colors are based on the jet color scheme within this range. A change in color from red to yellow to dark purple is therefore proportional to the change in the magnetic field strength. The multipolarity of 2 positive poles (red color) and 1 negative pole (dark purple color) of the heart's magnetic field is detected in a patient with inflammatory cardiomyopathy. *Second row*: The graphics show the vector change of the same subject as in the first row during immunosuppressive therapy. The initial MCG vector (left) is broad and wide in the second quadrant. After 3 days of immunosuppressive therapy, the vector becomes slimmer (panel in the middle). After nearly 3 weeks (right), the vector remains narrow and moves toward the first quadrant, a sign of therapy response. Changes of the vector correspond to changes in the magnetic field.

First, it can detect the magnetic field of the heart in a contactless manner without exposing the patient to radiation. Second, it is less affected by conductivity variations caused by lungs, skin, and muscles compared with ECG. With the help of multichannel systems,[21] the entire thoracic magnetic field can be assessed in one measurement.[21,22] Data can be obtained at rest within 60 seconds of measurement time.

In clinical applications, magnetocardiography has been mainly used for localization of cardiac arrhythmias[23–27] and for early diagnosis of myocardial ischemia.[28,29] Furthermore, early reports in literature have described its potential in detecting heart transplant rejection, suggesting a potential role in detecting myocardial inflammation.[30,31]

In our study, we used magnetocardiography as a screening method for inflammatory cardiomyopathy and to predict therapy response at an early stage of treatment.

METHODS

Data Availability

All data used for analyses in this study will be made available in a deidentified manner through Dr Bettina

Heidecker on request via email (bettina.heidecker@charite.de, corresponding author and study principal investigator). Data will be shared with academic staff only.

Because of privacy and ethical concerns, access to the data is restricted and cannot be made publicly available. Data were made available for the editor and peer reviewers during the review process.

Study Population and Study Design

In this prospective study, we evaluated the feasibility of using magnetocardiography as screening method to detect patients with inflammatory cardiomyopathy and its ability to monitor early treatment response compared with a current state-of-the-art approach, measurement of left ventricular ejection fraction (LVEF) by echocardiography. This study was approved by the ethics committee of the Charité Universitätsmedizin Berlin, Germany. All participants provided their written informed consent.

Patients admitted to our hospital during the period from January 2019 to January 2021 with newly diagnosed nonischemic cardiomyopathy and a control group without cardiomyopathy were enrolled. The group of patients without cardiomyopathy included healthy individuals as well as patients receiving medications for hypertension (eg, β-blocking agents or angiotensin-converting enzyme inhibitors). Furthermore, we enrolled 3 independent cohorts: (1) patients without inflammatory cardiomyopathy receiving immunosuppression; (2) patients with inflammatory cardiomyopathy without immunosuppressive therapy; and (3) patients with post–COVID-19 condition with neither inflammatory cardiomyopathy nor immunosuppressive therapy. Enrolled patients with post–COVID-19 condition did not show any signs or symptoms of inflammatory cardiomyopathy, and relevant laboratory parameters were within normal limits (high-sensitivity troponin T, CRP [C-reactive protein], N-terminal pro-B-type natriuretic peptide, and leukocytes). Post–COVID-19 condition was defined according to the official definition by the World Health Organization: "Post COVID-19 condition occurs in individuals with a history of probable or confirmed SARS-CoV-2 infection, usually 3 months from the onset of COVID-19 with symptoms that last for at least 2 months and cannot be explained by an alternative diagnosis. Common symptoms include fatigue, shortness of breath, cognitive dysfunction but also others […] which generally have an impact on everyday functioning." Definition available at https://www.who.int/publications/i/item/WHO-2019-nCoV-Post_COVID-19_condition-Clinical_case_definition-2021.1.

In addition, we tested diagnostic accuracy of magnetocardiography in a patient with myocarditis after mRNA vaccine against SARS-CoV-2.

Application of Magnetocardiography

In general, there is a low threshold for the use of magnetocardiography, as there are no known adverse effects for this technology. However, in patients with metal implants close to or within the heart, such as mechanical valves, internal cardioverter-defibrillators, or pacemakers, magnetocardiography measurements cannot be interpreted. Such devices could interfere with the magnetic field of a patient and compromise accurate measurements. Therefore, patients with such devices or implants were excluded from the study.

Diagnostic Workup

Diagnostic workup included history and physical examination, ECG, comprehensive laboratory testing based on differential diagnoses (complete blood cell count with differential, complete metabolic panel, CRP, ferritin, thyroid-stimulating hormone, antinuclear antibodies, antineutrophil cytoplasmic antibodies, soluble interleukin 2 receptor, serum electrophoresis, and immunofixation of serum and urine), genetic testing for M. Fabry or transthyretin amyloidosis variant, echocardiography, CMR, 99m Technetium labelled 3,3-diphosphono-1,2-propanodicarboxylic acid (99mTc-DPD) scintigraphy, or FDG-PET-CT. All patients diagnosed with inflammatory cardiomyopathy also underwent coronary angiography. Patients with coronary artery disease were excluded from the study.

EMB was performed in accordance with recommendations of the European Society of Cardiology.[5] Echocardiographic measurements were performed with the Vivid 8 Echocardiography instrument from GE.

Magnetocardiography Monitoring During Treatment

All patients underwent their first magnetocardiography and echocardiographic measurements at the time of diagnosis (ie, baseline measurement). If indicated, standard heart failure therapy with or without immunosuppression was initiated after baseline measurements based on current recommendations of the European Society of Cardiology.[5]

First, we sought to determine a magnetocardiography vector to detect cardiomyopathy in a primary cohort of 209 adult subjects. This cohort consisted of 66 subjects (32%) diagnosed with inflammatory cardiomyopathy, 17 (8%) diagnosed with cardiac amyloidosis, and 35 (17%) diagnosed with other types of nonischemic cardiomyopathy; 91 (44%) did not have cardiomyopathy. Diagnosis of cardiomyopathy was excluded on the basis of patient history, physical examination, and echocardiography.

The second analysis included 13 patients with inflammatory cardiomyopathy who underwent initiation

of immunosuppressive therapy after baseline magnetocardiography measurement.

Patients treated with immunosuppression had magnetocardiography and echocardiographic measurements at baseline and on days 7 and 30. Immunosuppressive therapy consisted of a daily oral dose of prednisolone 1 mg/kg total body weight for 2 weeks, with subsequent reduction of the total daily dose by 10 mg every 2 weeks. Positive treatment response under immunosuppressive therapy was defined as an improvement of LVEF from baseline to day 30 by at least 10%, similar to what has been used in prior literature.[32–34]

Finally, diagnostic accuracy of magnetocardiography was tested in 3 independent cohorts (total n=23) and 1 patient with vaccine-related myocarditis.

Patient Preparation for Magnetocardiography

Before undergoing a magnetocardiography measurement, patients had to take off any items that could potentially interfere with their intrinsic magnetic field, such as a wearable cardioverter-defibrillator or jewelry. Patients were placed in a supine position on a stretcher integrated into the magnetocardiography instrument (Figure 2). A standard 12-lead ECG was placed with magnetically compatible electrodes for rhythm monitoring.

The system used to measure the magnetic field was positioned in a contactless manner, ≈2 cm above the patient's thorax (Figure 2). Similarly to an ECG measurement, the patient is instructed not to move for 60 seconds of measurement.

Method of Magnetocardiography Measurements

Details on the method of magnetocardiography measurements are outlined in Data S1.

Statistical Analysis

Descriptive data are reported as mean (SD); change rates are reported with 95% CIs.

First, we evaluated the optimal threshold of a magnetocardiography vector to discriminate between patients with any subtype of cardiomyopathy versus subjects without cardiomyopathy. An optimal cut point value of the magnetocardiography vector was calculated in a binary classification task (ie, nonischemic cardiomyopathy versus no cardiomyopathy). For determining the optimal cut point value, we maximized the metric function and used the Youden index. The area under the receiver operating characteristic curve and Youden index were calculated to assess predictive performance of that threshold.

After testing the magnetocardiography vector as a diagnostic screening tool, we evaluated its ability to monitor treatment response. A decrease of the magnetocardiography vector by 10% toward normal on day 7 was used as an indicator for response to therapy. Given that there were no available data in the literature describing treatment response based on magnetocardiography vectors, estimation of effect size between groups could not be derived. We followed the well-established standard of 10% improvement of LVEF, as used in the literature.[32,33] We estimated that a sample size of at least 8 subjects is necessary to detect
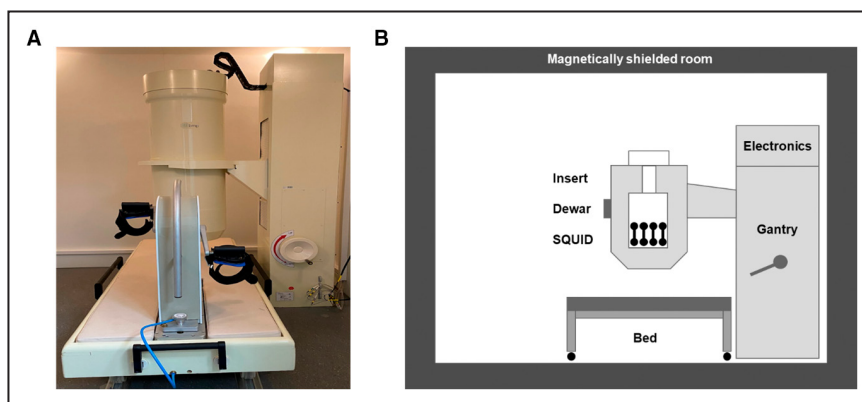

Figure 2. Display of the structure of the magnetocardiography (MCG) instrument (original and schematic).
A, On the left side is a photograph of the MCG instrument in its original size. MCG is a method to measure the heart's magnetic field without exposure to radiation. The vessel in the middle represents the dewar, the functional core of the MCG instrument. Subjects lie down on the stretcher, and the dewar is positioned over their chest without contact. **B**, On the right side is a schematic representation of the structure of the MCG instrument. The dewar contains the superconducting quantum interference device (SQUID) sensors that detect the heart's magnetic signals. The measurements are conducted in a magnetically shielded room to avoid deflection or other magnetic disturbances.

a difference in magnetocardiography vector and an improvement of LVEF by 10%, with a power of 80% and a significance level of 0.05. A 2-tailed $P<0.05$ was considered statistically significant.

To assess the effect of immunosuppressive therapy over time on outcomes (ie, magnetocardiography vector and LVEF at baseline before immunosuppressive therapy and at days 7 and 30 of treatment), we used linear mixed-effect models with an identity link function for normally distributed probability, as previously described.[35]

Each mixed model included time of repeated measurement as fixed effects while allowing intercepts to vary for each study subject (random-intercept model). Results are displayed, including F-statistics and degrees of freedom. Post hoc pairwise comparisons were Bonferroni corrected.

Finally, the pathologic threshold of the magnetocardiography vector was tested in 3 independent cohorts and a patient with vaccine-related myocarditis.

Statistical data analyses, tables, and graphs were generated using R (R Core Team, 2017).

RESULTS

In total, 233 patients were enrolled in this study (Figure 3). The mean age was 45 (±18) years, and 105 (45%) were women. For the primary proof-of-concept study, 209 adult subjects were enrolled between January 2019 and January 2021, of whom 66 subjects (32%) were diagnosed with inflammatory cardiomyopathy, 17 (8%) were diagnosed with cardiac amyloidosis, and 35 (17%) were diagnosed with other types of nonischemic cardiomyopathy; 91 (44%) did not have cardiomyopathy.

Among the 66 patients diagnosed with inflammatory cardiomyopathy, 13 were initiated on immunosuppressive therapy. Serial magnetocardiography measurements were obtained at baseline (before immunosuppression) and on days 7 and 30. On average, patients with inflammatory cardiomyopathy were aged 43 (±16) years, had a body mass index of 25.2 (±4.0) kg/m^2, and were predominantly men (69.2%). Subjects without cardiomyopathy were on average aged 36.3 (±14.5) years with a body mass index of 23.9 (±3.3) kg/m^2, and 50.5% were men (Table 1).

Exploratory Analysis: Definition of Optimal Cut Point Values for Magnetocardiography Vectors in Patients With Cardiomyopathy

An optimal cut point value of the magnetocardiography vector was calculated to discriminate between patients
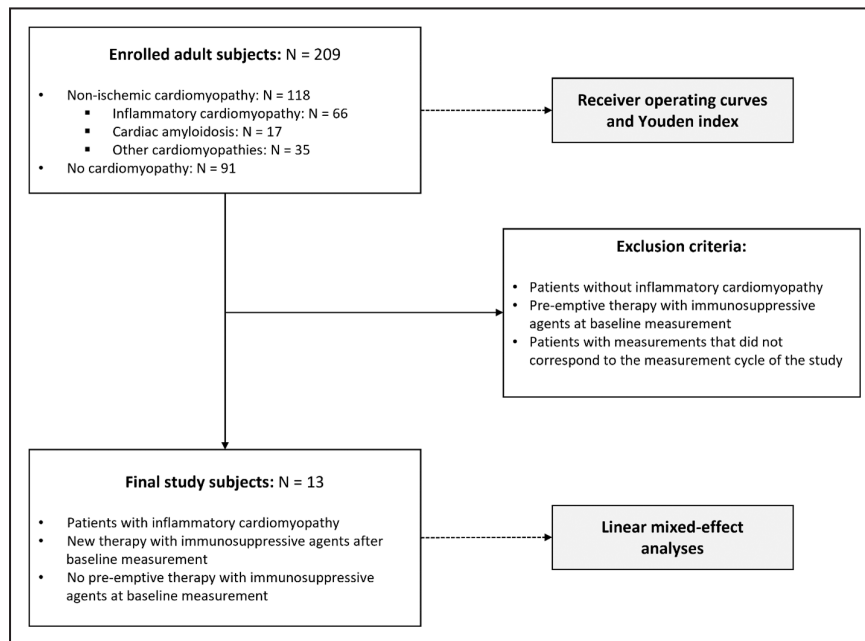

Figure 3. Study flow diagram of primary analysis.
In total, 233 patients were enrolled in this study. The primary analysis included 209 adult subjects, of whom 66 subjects (32%) were diagnosed with inflammatory cardiomyopathy, 17 (8%) were diagnosed with cardiac amyloidosis, and 35 (17%) were diagnosed with other types of nonischemic cardiomyopathy; 91 (44%) did not have cardiomyopathy. The second analysis included 13 patients with inflammatory cardiomyopathy, who underwent initiation of immunosuppressive therapy after baseline magnetocardiography (MCG) measurement. Finally, diagnostic accuracy of MCG was tested in 3 independent cohorts (total n=23) and 1 patient who developed myocarditis after COVID-19 vaccine.

Table 1. Characteristics of Patients Without Cardiomyopathy and With Inflammatory Cardiomyopathy

Characteristic	Patients without cardiomyopathy (N=91)	Patients with inflammatory cardiomyopathy (N=13)	Total (N=104)
Age, y	36.3 (14.5)	43.3 (15.6)	37.1 (14.8)
Sex			
Men	46 (50.5)	9 (69.2)	55 (52.9)
Women	45 (49.5)	4 (30.8)	49 (47.1)
Body mass index, kg/m^2	23.9 (3.31)	25.2 (3.97)	24.1 (3.40)
Magnetocardiography vector	0.0291 (0.0145)	0.104 (0.0573)	0.0385 (0.0345)
Ejection fraction, %	61.7 (2.75)	42.2 (14.2)	59.3 (8.50)
Left ventricular end-diastolic diameter, mm	46.4 (3.59)	51.6 (8.93)	47.0 (4.86)
β-Adrenergic receptor antagonists	1 (1.1)	11 (84.6)	12 (11.5)
Angiotensin-converting enzyme inhibitor	5 (5.5)	7 (53.8)	12 (11.5)
Sacubitril/valsartan	0 (0)	4 (30.8)	4 (3.8)
Diuretics	0 (0)	10 (76.9)	10 (9.6)

Numbers are displayed as mean (SD) or frequency (percentage).

with any type of nonischemic cardiomyopathy (N=118) and subjects without cardiomyopathy (N=91; Table 1) through analyses of area under the receiver operating characteristic curves. The optimal cut point value was defined at 0.051 (area under the curve, 0.78; sensitivity, 0.59; specificity, 0.95; positive predictive value,
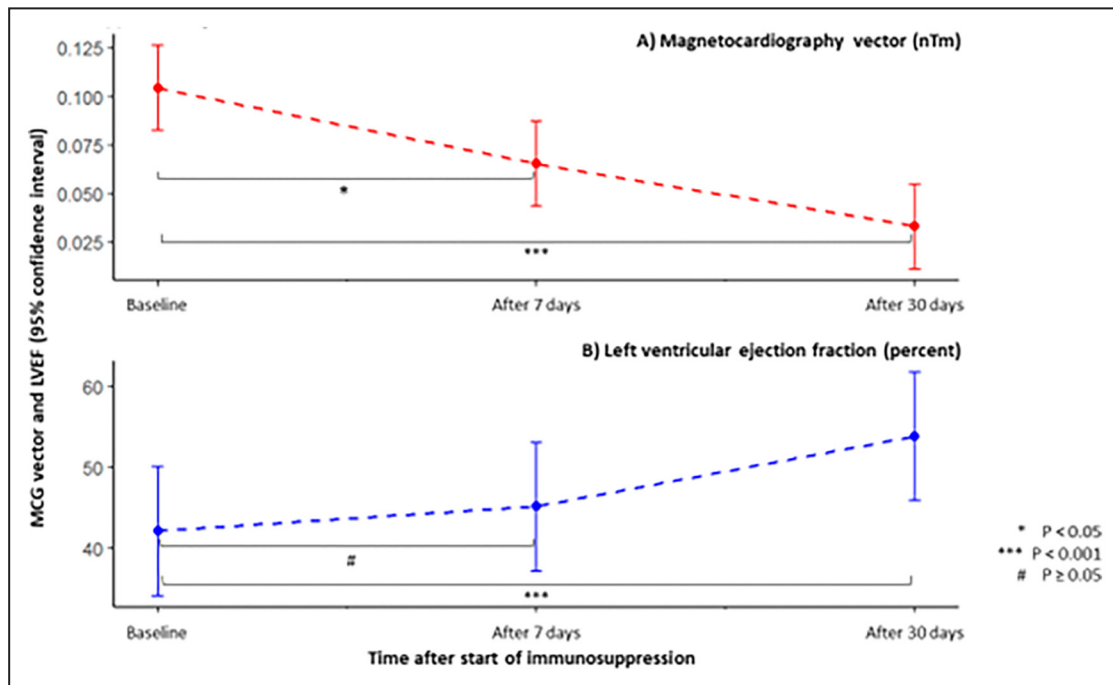

Figure 4. Magnetocardiography (MCG) vector and left ventricular ejection fraction (LVEF) at baseline and after 7 and 30 days of administering immunosuppressive agents.
A, MCG vector (changed significantly over time after administration of immunosuppressive agents; F [2, 24]=17.612; *P*<0.001). In particular, the MCG vector decreased from 0.10 (95% CI, 0.08–0.13) at baseline to 0.07 (95% CI, 0.04–0.09) within 7 days after administration of immunosuppressive agents (*P*=0.010). Within 30 days of administering immunosuppressants, the MCG vector decreased further to 0.03 (95% CI, 0.01–0.05); *P*<0.001 compared with baseline. **B**, LVEF (percentage) changed significantly over time after administration of immunosuppressive agents (F [2, 24]=19.31; *P*<0.001). However, within 7 days of administering immunosuppressive agents, change in left ventricular ejection fraction was not significant: 42.2% (95% CI, 34.2%–50.1%) at baseline vs 45.2% (95% CI, 37.2%–53.1%) after 7 days (*P*=0.414). Given 30 days of immunosuppressive therapy, left ventricular ejection fraction changed significantly to 53.8% (95% CI, 45.9%–61.8%); *P*<0.001 compared with baseline.

93.3%; and negative predictive value, 64%; Figure S4). We evaluated if there were subtype-specific magnetocardiography vectors for different cardiomyopathies: in subgroups of patients with inflammatory cardiomyopathy (N=66) and cardiac amyloidosis (N=17), optimal cut point values for the magnetocardiography vector were calculated at similar levels, at 0.051 and 0.052, respectively. Therefore, the magnetocardiography vector was able to identify a cardiomyopathy as abnormal, but it was not specific for subtypes of cardiomyopathy.

Early Detection of Treatment Response

The magnetocardiography vector changed significantly over time after administration of immunosuppressive agents in patients with inflammatory cardiomyopathy (F [2, 24]=17.612; $P<0.001$). In particular, the magnetocardiography vector decreased from 0.10 (95% CI, 0.08–0.13) at baseline to 0.07 (95% CI, 0.04–0.09) within 7 days after administration of immunosuppressive agents ($P=0.010$). Within 4 weeks of administering immunosuppressants, the magnetocardiography vector decreased further to 0.03 (95% CI, 0.01–0.05); $P<0.001$ compared with baseline (Figure 4A).

LVEF also changed significantly over time after administration of immunosuppressive agents (F [2, 24]=19.31; $P<0.001$). However, there was not a significant change in LVEF within 7 days of administering immunosuppressive agents: 42.2% (95% CI, 34.2%–50.1%) at baseline versus 45.2% (95% CI, 37.2%–53.1%) after 7 days ($P=0.414$). Only after 4 weeks of

immunosuppressive therapy, LVEF improved significantly to 53.8% (95% CI, 45.9%–61.8%); $P<0.001$ compared with baseline (Figure 4B).

Change in magnetocardiography vector compared with change in LVEF differed significantly from each other after 7 days of administering immunosuppressive agents: change in magnetocardiography vector −30.38% (±24.21%) versus change in LVEF 8.66% (±14.17%) ($P<0.001$) (Figure 5). Similarly, change in magnetocardiography vector compared with change in LVEF between 7 and 30 days of immunosuppressive therapy was significantly different: change in magnetocardiography vector −43.29% (±25.28%) versus change in LVEF 26.45% (±37.12%) ($P<0.001$) (Figure 5).

Examples of CMR images and their corresponding magnetocardiography vector from patients with inflammatory cardiomyopathy are illustrated in Figure 6.

Analyses of Diagnostic Accuracy in Independent Cohorts

To test diagnostic accuracy of the magnetocardiography vector in 3 independent cohorts, we evaluated patients receiving immunosuppression for conditions other than inflammatory cardiomyopathy (n=10), patients with inflammatory cardiomyopathy who were treated with standard heart failure therapy but without immunosuppression (n=4), and patients with post–COVID-19 condition who had neither signs nor symptoms of inflammatory cardiomyopathy and did not
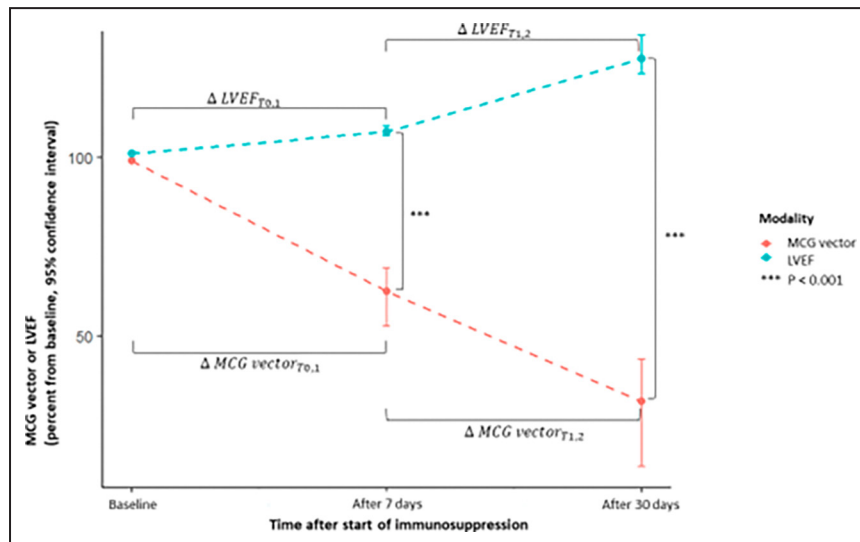

Figure 5. Magnetocardiography (MCG) vector and left ventricular ejection fraction (LVEF) at baseline and after 7 and 30 days of administering immunosuppressive agents (percentage from baseline).
Change in MCG vector (Δ MCG vector) compared with change in LVEF (Δ LVEF) differed significantly from each other after 7 days of administering immunosuppressive agents: Δ MCG vector −30.38% (±24.21%) vs Δ LVEF 8.66% (±14.17%) ($P<0.001$). Δ MCG vector compared with Δ LVEF after 30 days of immunosuppressive therapy: Δ MCG vector −43.29% (±25.28%) vs Δ LVEF 26.45% (±37.11%) ($P<0.001$).

receive any immunosuppressive therapy (n=9; Table 2). These patients were enrolled for independent testing after the proof-of-concept study was completed.

Clinical parameters of patients of the cohorts are illustrated in Table 2. Magnetocardiography vector analysis and measurement of ejection fraction by echocardiography were obtained in all 3 cohorts on day 1 of admission and 7 days later (Figure 7). The magnetocardiography vector in the cohort with inflammatory cardiomyopathy was abnormal (>0.051), whereas it was normal in the groups without inflammation (<0.051). There were no significant changes of the magnetocardiography vector or left ventricular ejection fraction between baseline and day 7.

Finally, we tested generalizability of the pathologic magnetocardiography vector in a 25-year-old man, who developed vaccine-related myocarditis after mRNA vaccine against SARS-CoV-2. Myocarditis was confirmed on the basis of clinical presentation, high-sensitivity troponin T, and CMR.

Indeed, magnetocardiography analysis correctly identified a pathologic magnetocardiography vector in this patient, similar to the average vector found in other patients with inflammatory cardiomyopathy of our cohort (Figure S5).

DISCUSSION

We present magnetocardiography as a practical, noninvasive screening method to detect inflammatory cardiomyopathy in patients in whom ischemic heart disease has been excluded, or in patients with low a priori probability of ischemic heart disease or other types of cardiac abnormality. In a recent study including 51 patients with coronary artery disease and 52 healthy volunteers, best sensitivity and specificity of magnetocardiography were 56% and 96%, respectively, revealing a similar diagnostic sensitivity as in our study for detecting cardiomyopathy in general.[36] Early reports in literature have suggested that
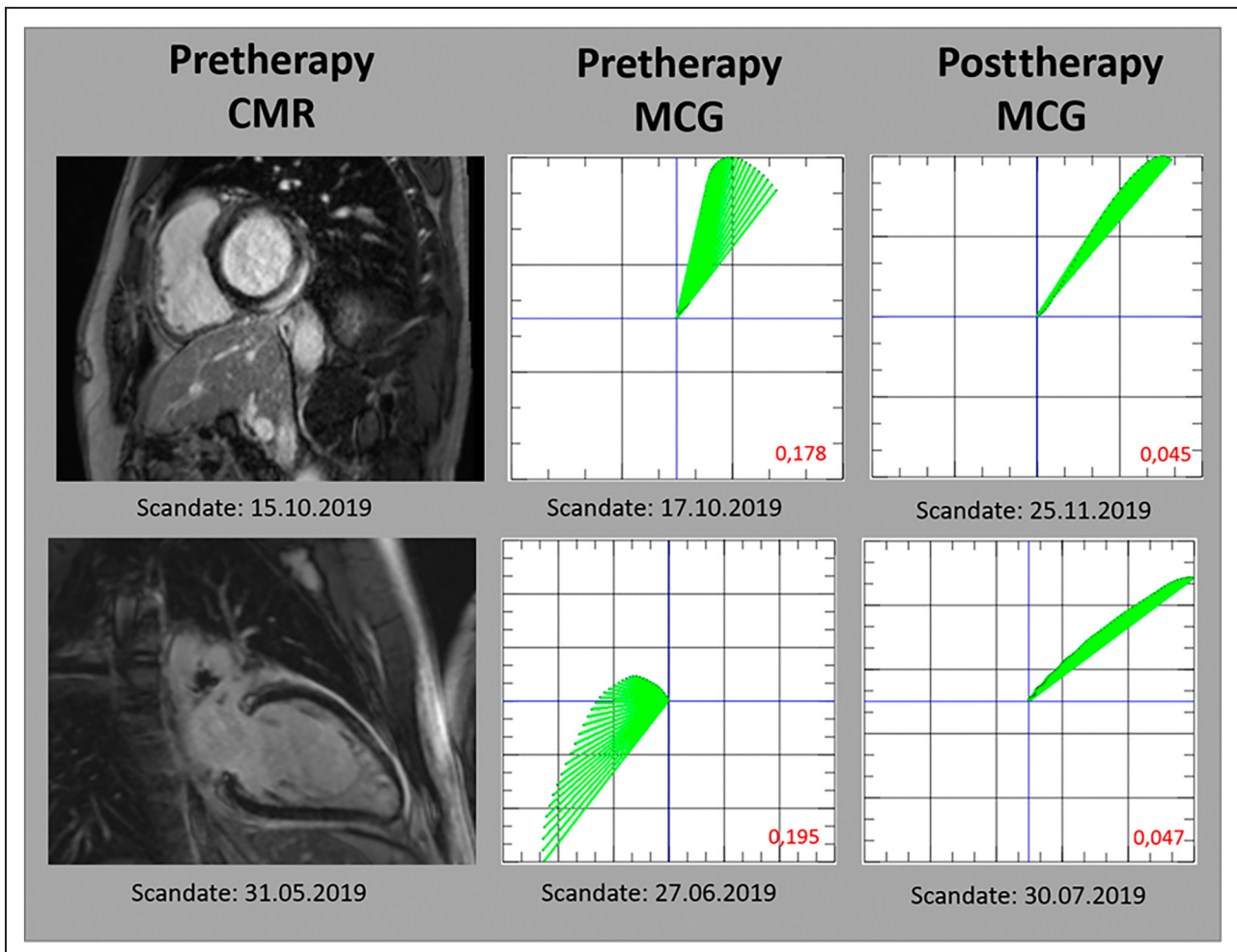

Figure 6.   Illustration of cardiac magnetic resonance imaging (CMR) from patients with inflammatory cardiomyopathy and their corresponding magnetocardiography (MCG) vector during therapy.
Each row illustrates the data of an individual patient. First column: CMR images of 2 patients with myocarditis; second and third columns: MCG vector at baseline and after approximately 1 month of anti-inflammatory therapy.

Table 2. Patient Characteristics of 3 Cohorts

Characteristic	Cohort 1: Immunosuppression and no inflammatory cardiomyopathy (N=10)	Cohort 2: Inflammatory cardiomyopathy and no immunosuppression (N=4)	Cohort 3: Post–COVID-19 condition, no inflammatory cardiomyopathy, and no immunosuppression (N=9)	Overall (N=23)
Age, y	50.3 (13.8)	28.8 (18.2)	46.3 (13.6)	45.0 (15.9)
Sex				
Men	4 (40.0)	3 (75.0)	2 (22.2)	9 (39.1)
Women	6 (60.0)	1 (25.0)	7 (77.8)	14 (60.9)
Body mass index, kg/m^2	26.9 (7.61)	27.3 (2.63)	23.8 (2.68)	25.7 (5.46)
Magnetocardiography vector				
Baseline	0.0321 (0.0134)	0.120 (0.0434)	0.0454 (0.0261)	0.0525 (0.0400)
At day 7	0.0281 (0.0116)	0.0915 (0.0341)	0.0294 (0.0190)	0.0397 (0.0306)
Ejection fraction, %				
Baseline	62.8 (1.81)	50.8 (12.3)	61.9 (4.76)	60.3 (7.11)
At day 7	63.1 (3.21)	52.8 (11.9)	63.3 (4.24)	61.4 (6.82)
Left ventricular end-diastolic diameter, mm				
Baseline	49.2 (4.78)	47.5 (6.45)	42.9 (7.29)	46 (6.57)
At day 7	49.2 (4.78)	48.3 (4.72)	45.9 (2.85)	47.9 (4.29)
β-Adrenergic receptor antagonists	1 (10.0)	3 (75.0)	0 (0)	4 (17.4)
Angiotensin-converting enzyme inhibitor	3 (30.0)	2 (50.0)	0 (0)	5 (21.7)
Sacubitril/valsartan	0 (0)	0 (0)	0 (0)	0 (0)
Diuretics	1 (10.0)	0 (0)	0 (0)	1 (4.3)

Numbers are displayed as mean (SD) or frequency (percentage).

magnetocardiography may be used to detect early myocardial inflammation in the setting of heart transplant rejection and myocarditis.[29–31] Although magnetocardiography was not able to discriminate different types of cardiomyopathy, our data suggest that magnetocardiography has the potential for broad diagnostic screening and measuring early treatment response to immunosuppression within 7 days in patients with inflammatory cardiomyopathy.

Given the fact that this diagnostic screening method has no known adverse effects and does not require much time or effort to perform, its application may lower the threshold to screen patients for inflammatory cardiomyopathy and improve the number of undetected cases consequently. Once an abnormal magnetocardiography vector is detected, additional diagnostic testing is required to evaluate whether the patient has inflammatory cardiomyopathy or another type of cardiomyopathy.

Patients with inflammatory cardiomyopathy under immunosuppression experienced an early decrease of the magnetocardiography vector toward normal.

The pathologic magnetocardiography vector was also tested in 3 independent cohorts who were either not treated with immunosuppression or received immunosuppression without having inflammatory cardiomyopathy. Inflammation was detected correctly in those patients, and no relevant changes in the magnetocardiography vector were detected within 7 days of standard therapy without immunosuppression.

With current state-of-the art diagnostic methods (echocardiography, FDG-PET-CT, and CMR), characterizing early treatment response to immunosuppression remains challenging. Echocardiography is a valuable tool to measure parameters such as ventricular function, intracardiac pressures, and valve function, without relevant adverse effects. While providing a broad range of valuable data that may guide treatment in patients with cardiomyopathies, echocardiography mostly measures indirect effects of inflammation-associated cardiac injury, such as wall motion abnormalities or impaired ventricular function. A delay in detection may lead to late allocation of appropriate therapies, at which point there may have already been partial damage of the myocardium. FDG-PET-CT directly measures the inflammatory metabolism of the heart. Although FDG-PET-CT is highly valuable in providing information about structural changes, as well as full extent and activity of inflammation during therapy, its clinical use is limited because of radiation exposure. CMR provides valuable structural and functional information about the heart and detects the effects of inflammation in inflammatory cardiomyopathy. Similar to
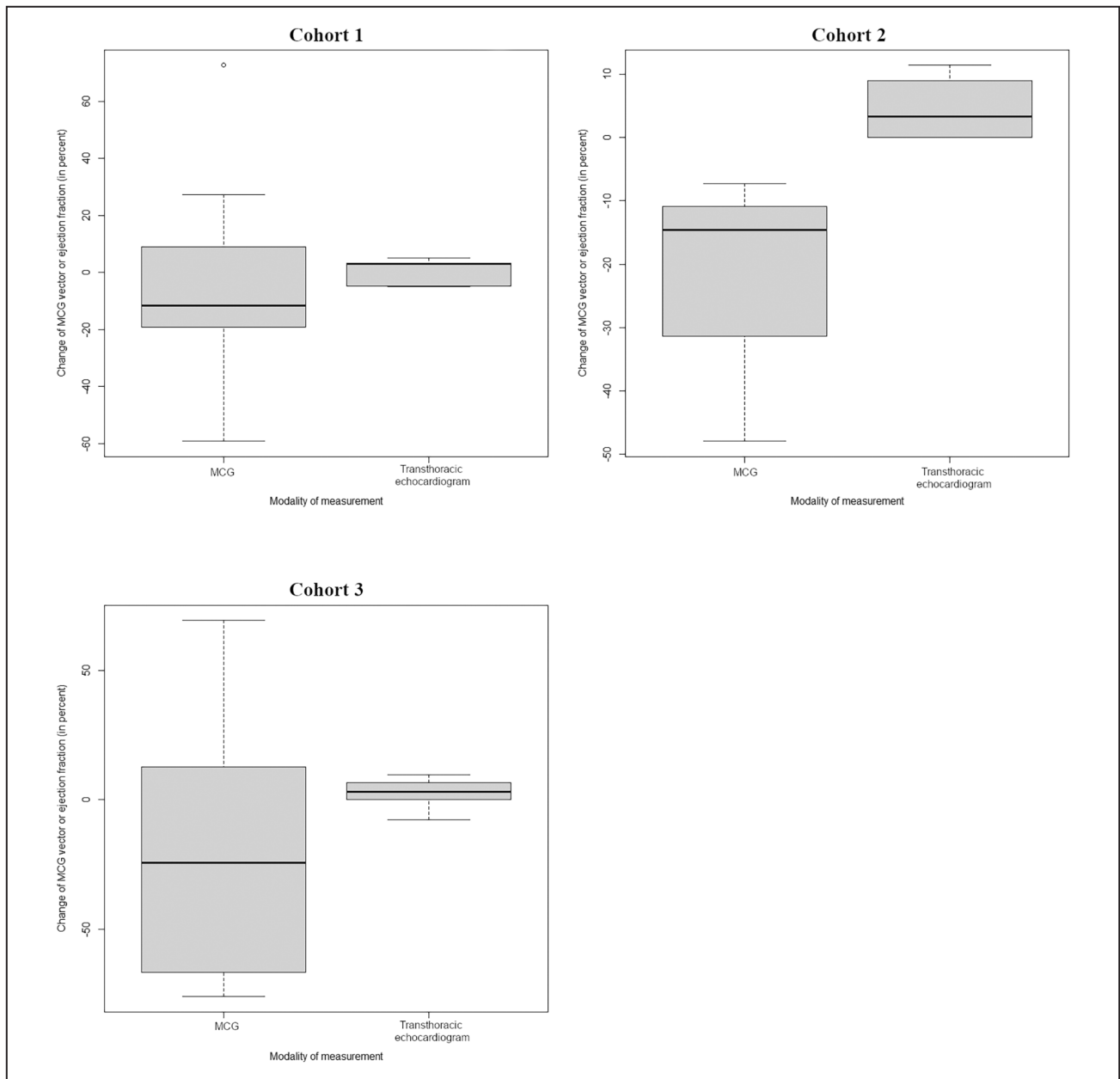
Figure 7.   Evaluation of the magnetocardiography (MCG) vector in 3 independent cohorts: change in MCG vector and left ventricular ejection fraction between baseline and 7 days.
Cohort 1: patients without inflammatory cardiomyopathy receiving immunosuppression (n=10). Cohort 2: patients with inflammatory cardiomyopathy not receiving immunosuppression (n=4). Cohort 3: patients with post–COVID-19 condition (n=9). The MCG vector in the cohort with inflammatory cardiomyopathy was abnormal (>0.051), whereas it was normal in the cohorts without inflammation (<0.051).

PET-CT, CMR cannot be applied frequently. Also, there has been cumulative evidence that gadolinium may get deposited in the brain when applied frequently during repeated CMR.[37] However, no adverse clinical effects have been demonstrated in the context of gadolinium deposition in the brain.[37] Diagnostic accuracy of CMR is estimated at ≈80%.[38] EMB is the gold standard in diagnosing inflammatory cardiomyopathy and a prerequisite for initiation of immunosuppressive therapy.[3]

Although the risk for complications during an EMB is overall low,[12] the cumulative risk would increase considerably if performed repetitively within short intervals in the same patient. Therefore, although important for initial diagnosis, EMB is rarely obtained in frequent intervals in patients undergoing immunosuppressive therapy for inflammatory cardiomyopathy. Although these state-of-the art methods for diagnosis and monitoring of treatment response are crucial for the care of

patients with inflammatory cardiomyopathy, we saw a clinical need to develop a complementary method that supports the early detection of inflammatory cardiomyopathy and response to immunosuppressive therapy.

Although the specificity of an abnormal magnetocardiography vector was high (95%) for detection of cardiomyopathy of any kind, its sensitivity was rather low (59%). Also, magnetocardiography was not able to discriminate between different types of cardiomyopathy. However, all patients with inflammatory cardiomyopathy had an abnormal magnetocardiography vector. Furthermore, magnetocardiography analysis was able to detect myocarditis after mRNA vaccine against SARS-CoV-2. Although myocarditis after mRNA vaccines is rare,[39] our data suggest that magnetocardiography could be a valuable screening tool in this still poorly understood adverse event.

Our findings describing a shift in the magnetocardiography vector, in particular in patients with inflammatory cardiomyopathy, are biologically plausible. From a physics perspective, all magnetic fields are created by moving electrons. We speculate that the inflammation may change the trajectories of the moving electrons, the number of electrons that are moving, or both. It has been well established that inflammation may lead to acidosis, which could affect movement of ions because of changes in charge. The trajectory of ions may also be affected by changes in the structure or the contractile behavior of the heart, resulting from inflammation.

Taken together, our findings suggest that the magnetocardiography vector is a valuable screening method for inflammatory cardiomyopathy and behaves similarly to a tumor marker.[40,41] Its value does not lie primarily in diagnosing a specific disease, but in reflecting therapy response accurately and early, thereby providing the physician with an additional tool to individualize therapy.

Finally, it warrants mentioning that in some patients of our cohort the magnetocardiography vector findings positively affected patient management. In 3 patients with inflammatory cardiomyopathy, detection of a worsening magnetocardiography vector during clinical follow-up led to additional diagnostic imaging, including PET-CT or CMR, which detected worsening inflammation and led to escalation of immunosuppressive therapy with subsequent improvement of the patient's clinical condition.

Limitations

A limitation of this study is its small sample size. As we conducted this study in a tertiary care center with a wide referral range (up to 700 km), not all patients with inflammatory cardiomyopathy who were placed on immunosuppression were able to present for follow-up at 7 and 30 days. Therefore, those patients could not be included in the main proof-of-concept analysis. Also, patients with metal-containing implants in the chest could not be included in this study. However, results were highly consistent among patients who were able to participate.

CONCLUSIONS

Magnetocardiography is a method without known adverse effects with the ability to identify an abnormal magnetic field. To the best of our knowledge, this is the first study investigating the magnetocardiography vector in the setting of inflammatory cardiomyopathy and using it for diagnostic screening and for monitoring early response to therapy. Magnetocardiography is a noninvasive measurement that can be obtained within 60 seconds. In our study, we have demonstrated that treatment response to immunosuppressive therapy can be detected within 7 days in patients with inflammatory cardiomyopathy, whereas echocardiographic improvement was detectable only after 30 days in patients responding to therapy. The change in magnetocardiography vector was highly significant (effect size: 30%) on day 7 of immunosuppressive therapy. Given the high sensitivity of magnetocardiography in detecting clinical improvement, we suggest that the application of magnetocardiography in patients undergoing immunosuppressive therapy for inflammatory cardiomyopathy may be a valuable addition to current state-of-the-art methods of measuring treatment response.

REFERENCES

1. Felker GM, Thompson RE, Hare JM, Hruban RH, Clemetson DE, Howard DL, Baughman KL, Kasper EK. Underlying causes and long-term survival in patients with initially unexplained cardiomyopathy. *N Engl J Med*. 2000;342:1077–1084. doi: 10.1056/NEJM20000413342 1502

2. Tschope C, Ammirati E, Bozkurt B, Caforio ALP, Cooper LT, Felix SB, Hare JM, Heidecker B, Heymans S, Hubner N, et al. Myocarditis and inflammatory cardiomyopathy: current evidence and future directions. *Nat Rev Cardiol*. 2021;18:169–193. doi: 10.1038/s41569-020-00435-x

3. Heidecker BCL. Acute Fulminant Myocarditis. In: Brown DL, ed. *Cardiac Intensive Care*. 3rd ed. Elsevier; 2019:199–204.

4. Cooper LT Jr, Berry GJ, Shabetai R. Idiopathic giant-cell myocarditis—natural history and treatment. Multicenter Giant Cell Myocarditis Study Group Investigators. *N Engl J Med*. 1997;336:1860–1866. doi: 10.1056/NEJM199706263362603

5. Caforio AL, Pankuweit S, Arbustini E, Basso C, Gimeno-Blanes J, Felix SB, Fu M, Helio T, Heymans S, Jahns R, et al. Current state of knowledge on aetiology, diagnosis, management, and therapy of myocarditis: a position statement of the European Society of Cardiology Working Group on Myocardial and Pericardial Diseases. *Eur Heart J*. 2013;34:2636–2648. 2648a-2648d. doi: 10.1093/eurheartj/eht210

6. Merken J, Hazebroek M, Van Paassen P, Verdonschot J, Van Empel V, Knackstedt C, Abdul Hamid M, Seiler M, Kolb J, Hoermann P, et al. Immunosuppressive therapy improves both short- and long-term prognosis in patients with virus-negative nonfulminant inflammatory cardiomyopathy. *Circ Heart Fail*. 2018;11:e004228. doi: 10.1161/CIRCHEARTFAILURE.117.004228

7. Sadek MM, Yung D, Birnie DH, Beanlands RS, Nery PB. Corticosteroid therapy for cardiac sarcoidosis: a systematic review. *Can J Cardiol*. 2013;29:1034–1041. doi: 10.1016/j.cjca.2013.02.004

8. Nagai S, Yokomatsu T, Tanizawa K, Ikezoe K, Handa T, Ito Y, Ogino S, Izumi T. Treatment with methotrexate and low-dose corticosteroids in sarcoidosis patients with cardiac lesions. *Intern Med*. 2014;53:2761. doi: 10.2169/internalmedicine.53.3120

9. Berg J, Kottwitz J, Baltensperger N, Kissel CK, Lovrinovic M, Mehra T, Scherff F, Schmied C, Templin C, Luscher TF, et al. Cardiac magnetic resonance imaging in myocarditis reveals persistent disease activity despite normalization of cardiac enzymes and inflammatory parameters at 3-month follow-up. *Circ Heart Fail*. 2017;10:e004262. doi: 10.1161/CIRCHEARTFAILURE.117.004262

10. Heidecker B, Williams SH, Jain K, Oleynik A, Patriki D, Kottwitz J, Berg J, Garcia JA, Baltensperger N, Lovrinovic M, et al. Virome sequencing in patients with myocarditis. *Circ Heart Fail*. 2020;13:e007103. doi: 10.1161/CIRCHEARTFAILURE.120.007103

11. Chow LH, Radio SJ, Sears TD, McManus BM. Insensitivity of right ventricular endomyocardial biopsy in the diagnosis of myocarditis. *J Am Coll Cardiol*. 1989;14:915–920. doi: 10.1016/0735-1097(89)90465-8

12. Holzmann M, Nicko A, Kuhl U, Noutsias M, Poller W, Hoffmann W, Morguet A, Witzenbichler B, Tschope C, Schultheiss HP, et al. Complication rate of right ventricular endomyocardial biopsy via the femoral approach: a retrospective and prospective study analyzing 3048 diagnostic procedures over an 11-year period. *Circulation*. 2008;118:1722–1728. doi: 10.1161/CIRCULATIONAHA.107.743427

13. Baule G, McFee R. Detection of the magnetic field of the heart. *Am Heart J*. 1963;66:95–96. doi: 10.1016/0002-8703(63)90075-9

14. Wacker-Gussmann A, Strasburger JF, Wakai RT. Fetal magnetocardiography alters diagnosis and management in fetal congenital heart disease and cardiomyopathy. *JACC Clin Electrophysiol*. 2022;8:1159–1161. doi: 10.1016/j.jacep.2022.04.012

15. Wacker-Gussmann A, Strasburger JF, Wakai RT. Contribution of fetal magnetocardiography to diagnosis, risk assessment, and treatment of fetal arrhythmia. *J Am Heart Assoc*. 2022;11:e025224. doi: 10.1161/JAHA.121.025224

16. Arai K, Kuwahata A, Nishitani D, Fujisaki I, Matsuki R, Nishio Y, Xin Z, Cao X, Hatano Y, Onoda S, et al. Millimetre-scale magnetocardiography of living rats with thoracotomy. *Commun Phys*. 2022;5:200. doi: 10.1038/s42005-022-00978-0

17. Tolstrup K, Madsen BE, Ruiz JA, Greenwood SD, Camacho J, Siegel RJ, Gertzen HC, Park JW, Smars PA. Non-invasive resting magnetocardiographic imaging for the rapid detection of ischemia in subjects presenting with chest pain. *Cardiology*. 2006;106:270–276. doi: 10.1159/000093490

18. Alday EA, Ni H, Zhang C, Colman MA, Gan Z, Zhang H. Comparison of electric- and magnetic-cardiograms produced by myocardial ischemia in models of the human ventricle and torso. *PLoS One*. 2016;11:e0160999. doi: 10.1371/journal.pone.0160999

19. Agarwal R, Saini A, Alyousef T, Umscheid CA. Magnetocardiography for the diagnosis of coronary artery disease: a systematic review and meta-analysis. *Ann Noninvasive Electrocardiol*. 2012;17:291–298. doi: 10.1111/j.1542-474X.2012.00538.x

20. Holland RP, Brooks H. Precordial and epicardial surface potentials during myocardial ischemia in the pig. A theoretical and experimental analysis of the TQ and ST segments. *Circ Res*. 1975;37:471–480. doi: 10.1161/01.RES.37.4.471

21. Moshage W, Weikl A, Abraham-Fuchs K, Schneider S, Bachmann K, Reichenberger H. Magnetocardiography: technical progress by a multichannel SQUID system. *Biomed Tech (Berl)*. 1989;34:205–206. doi: 10.1515/bmte.1989.34.s1.205

22. Moshage W, Achenbach S, Weikl A, Gohl K, Bachmann K, Abraham-Fuchs K, Harer W, Schneider S. Clinical magnetocardiography: experience with a biomagnetic multichannel system. *Int J Card Imaging*. 1991;7:217–223. doi: 10.1007/BF01797754

23. Fenici R, Melillo G. Magnetocardiography: ventricular arrhythmias. *Eur Heart J*. 1993;14:53–60.

24. Batie M, Bitant S, Strasburger JF, Shah V, Alem O, Wakai RT. Detection of fetal arrhythmia using optically-pumped magnetometers. *JACC Clin Electrophysiol*. 2018;4:284–287. doi: 10.1016/j.jacep.2017.08.009

25. Cuneo BF, Strasburger JF, Yu S, Horigome H, Hosono T, Kandori A, Wakai RT. In utero diagnosis of long QT syndrome by magnetocardiography. *Circulation*. 2013;128:2183–2191. doi: 10.1161/CIRCULATIONAHA.113.004840

26. Schmitz L, Brockmeier K, Trahms L, Erné SN. Magnetocardiography in patients with cardiomyopathy and operated congenital heart disease. In: Williamson SJ, Hoke M, Stroink G, Kotani M, eds. *Advances in Biomagnetism*. Springer US; 1989:453–456. doi: 10.1007/978-1-4613-0581-1_97

27. Fenici RR, Melillo G, Masselli M. Clinical magnetocardiography. *Int J Cardiac Imaging*. 1991;7:151–167. doi: 10.1007/BF01797748

28. Hailer B, Van Leeuwen P. Detection of coronary artery disease with MCG. *Neurol Clin Neurophysiol*. 2004;2004:82.

29. IC VS, Stadnyuk L, Miasnykov G, Kazmirchyk A, Sosnytska T, Gurjeva O. Magnetocardiography capabilities in myocardium injuries diagnosis. *World J Cardiovasc Dis*. 2013;3:380. doi: 10.4236/wjcd201335059

30. Schmitz L, Koch H, Brockmeier K, Mueller JM, Schueler SM, Warnecke H, Hetzer R, Erné S. Magnetocardiographic diagnosis of graft rejection after heart transplantation. Proceedings of the 8th International Conference of Biomagnetism. 1991;8.

31. Achenbach S, Moshage W, Graf S, Bachmann K and Permanetter B. Magnetocardiographic parameters for the detection of graft rejection after heart transplantation. 1995;40:303–304.

32. Singh JP, Solomon SD, Fradley MG, Barac A, Kremer KA, Beck CA, Brown MW, McNitt S, Schleede S, Zareba W, et al. Association of cardiac resynchronization therapy with change in left ventricular ejection fraction in patients with chemotherapy-induced cardiomyopathy. *JAMA*. 2019;322:1799–1805. doi: 10.1001/jama.2019.16658

33. Solomon SD, Foster E, Bourgoun M, Shah A, Viloria E, Brown MW, Hall WJ, Pfeffer MA, Moss AJ, Investigators M-C. Effect of cardiac resynchronization therapy on reverse remodeling and relation to outcome: multicenter automatic defibrillator implantation trial: cardiac resynchronization therapy. *Circulation*. 2010;122:985–992. doi: 10.1161/CIRCULATIONAHA.110.955039

34. Bozkurt B, Coats AJ, Tsutsui H, Abdelhamid M, Adamopoulos S, Albert N, Anker SD, Atherton J, Bohm M, Butler J, et al. Universal definition and classification of heart failure: a report of the heart failure society of America, heart failure association of the European Society of Cardiology, Japanese Heart Failure Society and Writing Committee of the Universal Definition of Heart Failure. *J Card Fail*. 2021;27:387–413.

35. Thevathasan T, Grabitz SD, Santer P, Rostin P, Akeju O, Boghosian JD, Gill M, Isaacs L, Cotten JF, Eikermann M. Calabadion 1 selectively reverses respiratory and central nervous system effects of fentanyl in a rat model. *Br J Anaesth*. 2020;125:e140–e147. doi: 10.1016/j.bja.2020.02.019

36. Fenici R, Brisinda D. Predictive value of rest magnetocardiography in patients with stable angina. *Int Congr Ser*. 2007;1300:737–740. doi: 10.1016/j.ics.2007.02.022

37. Gulani V, Calamante F, Shellock FG, Kanal E, Reeder SB; International Society for Magnetic Resonance in Medicine. Gadolinium deposition in the brain: summary of evidence and recommendations. *Lancet Neurol*. 2017;16:564–570. doi: 10.1016/S1474-4422(17)30158-8

38. Friedrich MG, Sechtem U, Schulz-Menger J, Holmvang G, Alakija P, Cooper LT, White JA, Abdel-Aty H, Gutberlet M, Prasad S, et al. Cardiovascular magnetic resonance in myocarditis: a JACC White Paper. *J Am Coll Cardiol*. 2009;53:1475–1487. doi: 10.1016/j.jacc.2009.02.007

39. Barda N, Dagan N, Ben-Shlomo Y, Kepten E, Waxman J, Ohana R, Hernan MA, Lipsitch M, Kohane I, Netzer D, et al. Safety of the BNT162b2 mRNA Covid-19 vaccine in a nationwide setting. *N Engl J Med*. 2021;385:1078–1090. doi: 10.1056/NEJMoa2110475

40. Riedinger JM, Bonnetain F, Basuyau JP, Eche N, Larbre H, Dalifard I, Wafflart J, Ricolleau G, Pichon MF. Change in CA 125 levels after the first cycle of induction chemotherapy is an independent predictor of epithelial ovarian tumour outcome. *Ann Oncol*. 2007;18:881–885. doi: 10.1093/annonc/mdl500

41. Ebeling FG, Stieber P, Untch M, Nagel D, Konecny GE, Schmitt UM, Fateh-Moghadam A, Seidel D. Serum CEA and CA 15-3 as prognostic factors in primary breast cancer. *Br J Cancer*. 2002;86:1217–1222. doi: 10.1038/sj.bjc.6600248

42. Baule GM, McFee R. The magnetic heart vector. *Am Heart J*. 1970;79:223–236. doi: 10.1016/0002-8703(70)90312-1

43. Kandori A, Ogata K, Miyashita T, Watanabe Y, Tanaka K, Murakami M, Oka Y, Takaki H, Hashimoto S, Yamada Y, et al. Standard template of adult magnetocardiogram. *Ann Noninvasive Electrocardiol*. 2008;13:391–400. doi: 10.1111/j.1542-474X.2008.00246.x

44. Nousiainen J, Oja S, Malmivuo J. Normal vector magnetocardiogram. II. Effect of constitutional variables. *J Electrocardiol*. 1994;27:233–241. doi: 10.1016/S0022-0736(94)80007-3

45. Nousiainen J, Oja S, Malmivuo J. Normal vector magnetocardiogram. I. Correlation with the normal vector ECG. *J Electrocardiol*. 1994;27:221–231. doi: 10.1016/S0022-0736(94)80006-5

SUPPLEMENTAL MATERIAL

Data S1.

Supplemental Methods

Methodology of MCG measurements

Action potentials of the heart muscle cells create ion currents that cause voltage fluctuations between energized and de-energized tissue and thereby create a magnetic field (42). Biomagnetic signals are in the range of 10^{-15} to 10^{-11} Tesla. Thus, they are weaker than the earth's magnetic field by order of 10^{-6}. These signals can be measured by sensitive magnetic field sensors, called SQUIDs (Superconducting Quantum Interference Sensors). These SQUIDS reach their supra-conducting habit at a temperature of 4,2 K (-269°), which needs a cooling with liquid helium in a vacuum jacket vessel, called Dewar.

The measurement requires a magnetically shielded room (MSR) and a 1st order gradiometer to avoid electromagnetic interference with the magnetic field of the human heart.

This field is measured by using 64-channels (CS-MAG III, Biomagnetik Park GmbH, Hamburg, Germany).

MCG can detect three independent components (x, y, z component) of the magnetic field (43). The z-axis is perpendicular to the chest plane. With respect to the z component, the x-y axis follows the right-hand rule. The y-axis for example is orientated to the patient's head (Figure S1). The MCG system consists of 16 axial and 48 tangential (24 in x and 24 in y direction) superconducting quantum interference device (SQUID) sensors. The system has a sensitivity of <6.5 fTrms/√ Hz over 100 Hz.

The data from the 64-channels is averaged and filtered with a bandpass. By using an adjustment of the zero lines and evaluating the R-wave position automatically, it ends up having an interference-free and high-resolution MCG.

The software (Cardio Expert 2.5) automatically calculates minimum-, maximum- and summation-value from all 64-channels for the different parameters (Figure S1).

The software consists of control, acquisition, signal processing and analysis function. The control software (SW) controls the SQUID operation by optimizing the operating parameters (bias current, feedback flux, offset voltage in the flux-locked loop circuit, integrator on/off) and analog filters. The acquisition SW displays MCG signals simultaneously. Then signal processing including baseline correction, digital filtering (high-pass, low-pass, DC notch), and averaging function are included. The averaged signals are analyzed after using a baseline correction. The baseline correction calculates and corrects the isoline of the signal consisting of a significant but low-frequency disturbance of the magnetic flux density using a mathematical algorithm.

We analyzed different time intervals from the QRS-complex to the T-wave maximum.

The rationale of measuring vectors in magnetocardiography (VMCG) is similar to the measurement of the vector in a 12-lead ECG (VECG) (44, 45).

Vector Magnetocardiography (VMCG) is a similar method to VECG (see Nousiainen, Oja, Mailmivuo, 1994) (44, 45).

The VMCG gives a robust and stable solution to calculate and illustrate the direction and amplitude of the electric current of the heart. One way of representing the VMCG is as a trace of the sinus rhythm, where each segment of the trace points from the previous current vector to the next current vector. It is then possible to observe angle and amplitude variations over an entire heartbeat in a single picture (like a current field map).

In total, four options are available (referring to terms as used in an ECG): From P-beg to T-end, from QRS-end to T-max, from RT-half to T-max, from T-beg to T-max, from P-beg to T-end. In our case, we focused on the loop of T-beg to T-max.

For this, the VMCG calculates MCG vector trajectories and displays them in 3-dimensional planes (Figure S2). In other words, we are analyzing the time dependent orientation or path of

calculated pseudo current. Therefore, we used various parameters for a geometric quantification:

The normalized area of the T-wave loop is calculated with Heron's formula, since this formula (see Wikipedia, https://en.wikipedia.org/wiki/Heron%27s_formula) returns the area of a triangle.

Further, the T-distance from T-beg to T-max is calculated as the distance between start and end point of the maximum current density.

The start end ratio is also calculated. That means the ratio of a vector pointing from T-beg to T-max interval by a vector pointing from end to the same point.

Figure S1: Sensor Type 2
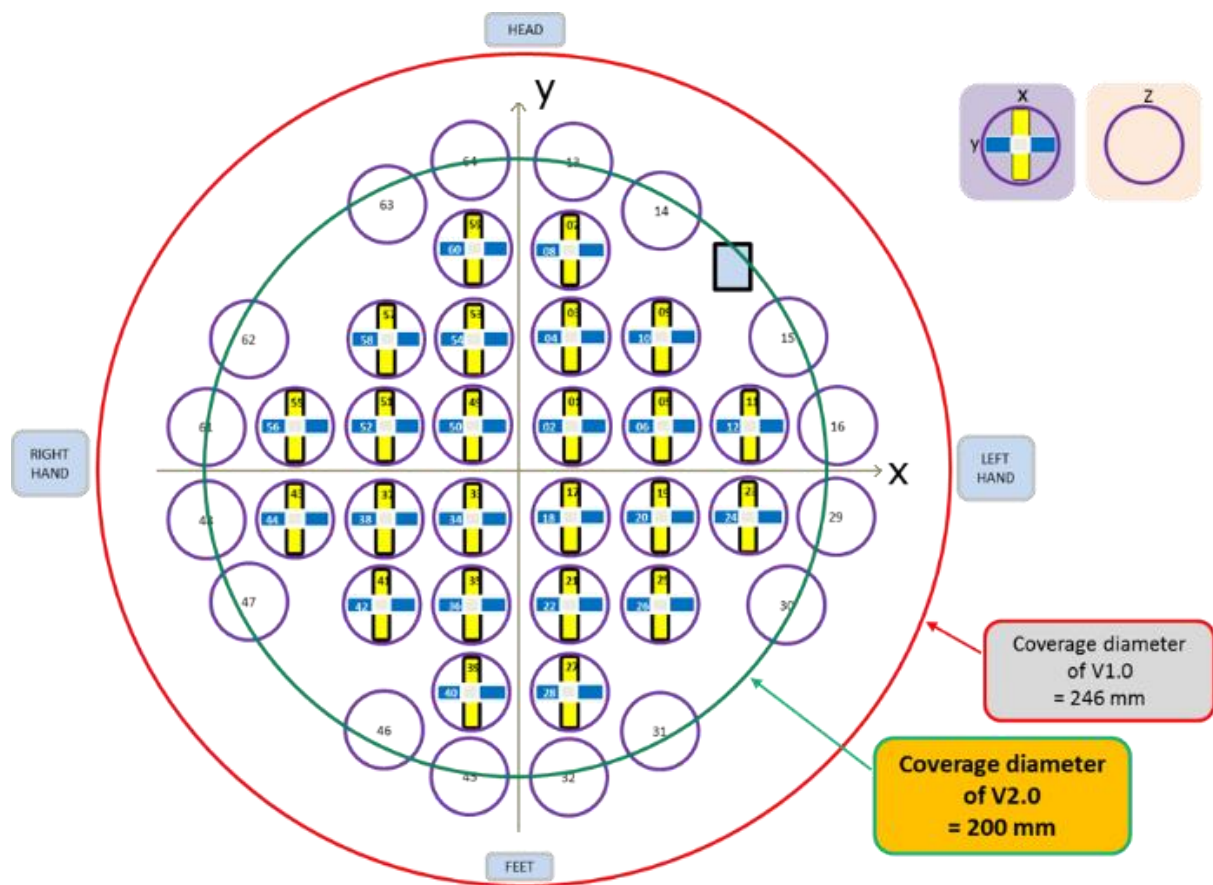
	Summary table
System sensitivity	<6.5 fTrms/$\sqrt{Hz}$ over 100 Hz
Typical signal strength	10 pT (pico Tesla)
Range of time averaging intervals used	45 seconds
Bandpass filtering interval used	0.5Hz to 100Hz
Notchfilter	@50Hz
Number of times each patient was tested	3

Figure S2: Visualization of VMCG. The normalized area of the T-wave loop can be calculated with help of Heron's formula (e.g., see Wikipedia). A large area indicates a sick patient.
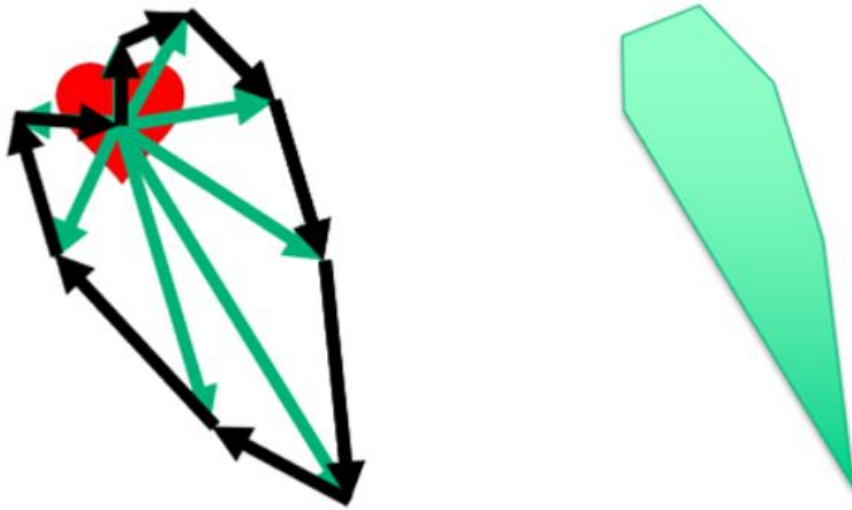
Figure S3: Exemplary graphical outputs of vectors in magnetocardiography

a. On the left side is an exemplary graphical output of a normal vector in magnetocardiography (MCG) in green from a subject without inflammatory cardiomyopathy. The vector represents the measured area from the beginning of the T-wave until the maximum of T-wave. A slim surface area and vector position in the first quadrant (1) between 0° and 90° are considered normal.

b. On the right side is an exemplary graphical output of a subject with inflammatory cardiomyopathy. A broader, larger surface area of the vector and the second quadrant positioning are considered pathological.
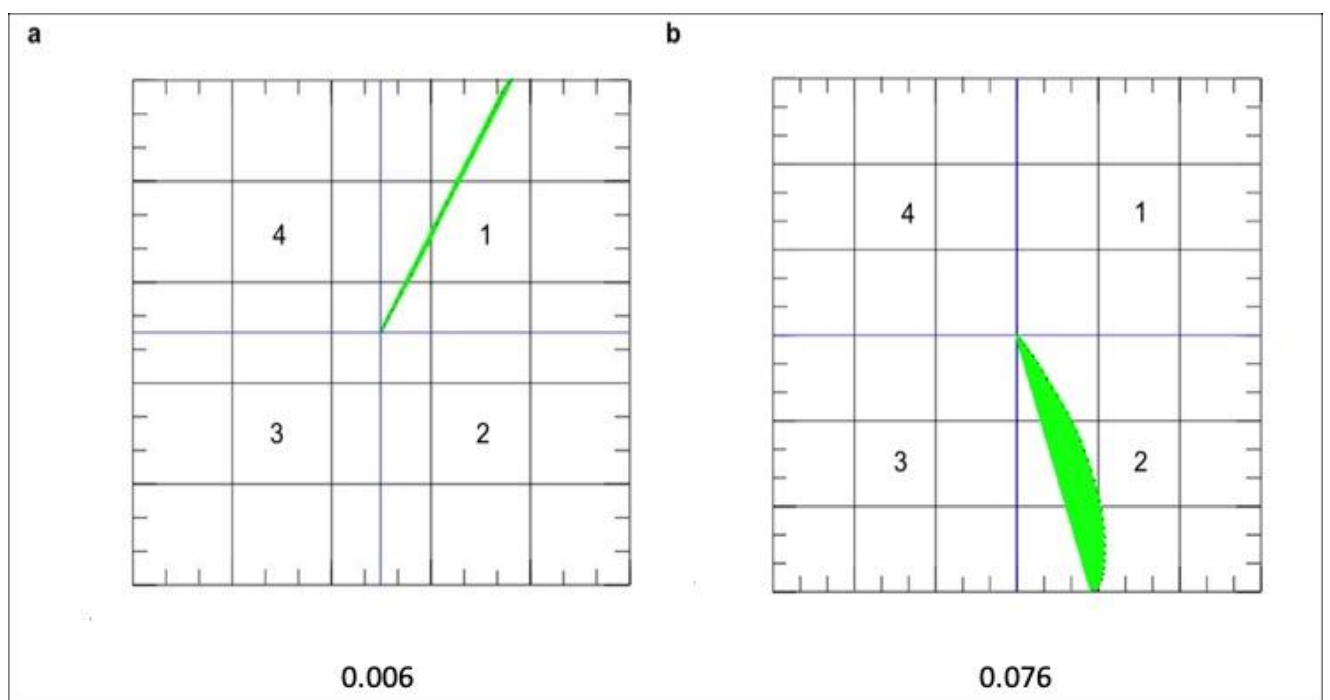
Figure S4: Area under receiver operating curve and "optimal" cutpoint estimation for magnetocardiography (MCG) vector.

The area under the receiver operating curve (ROC) and Youden index were calculated to assess the predictive performance and "optimal" threshold of the MCG vector to discriminate between patients with any subtype of non-ischemic cardiomyopathy (N = 118) versus subjects without cardiomyopathy (N = 91). The optimal cut-point value for the MCG vector was defined at 0.051. The area under the ROC curve was 0.78, sensitivity was 59% and specificity was 95%.
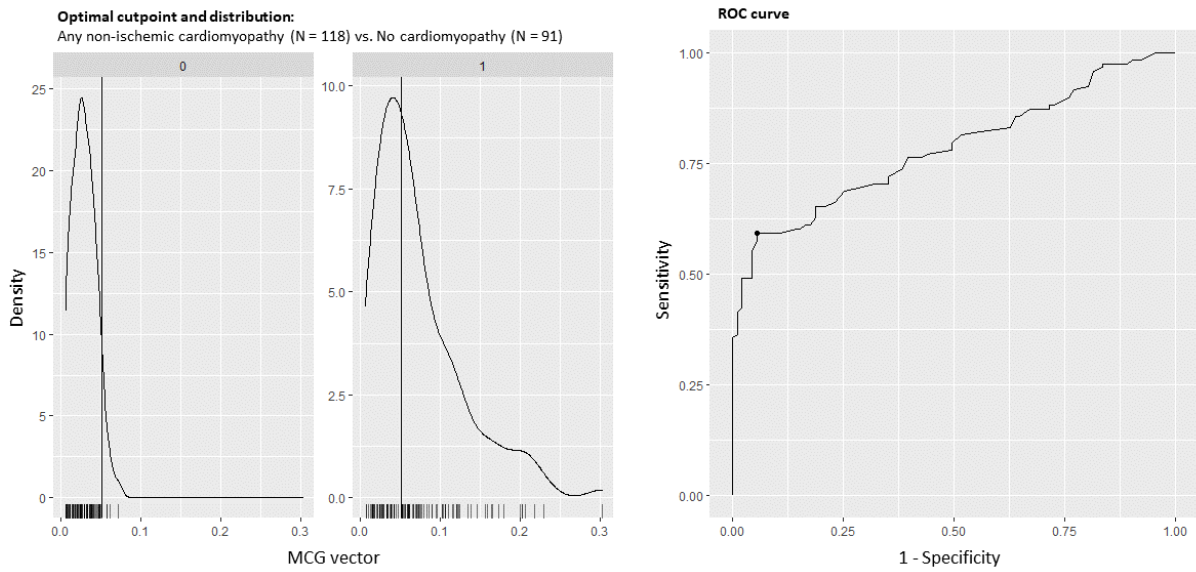
Figure S5: Comparison of graphical output of magnetocardiography vectors in a patient with inflammatory cardiomyopathy (a), and a patient who developed myocarditis after an mRNA vaccine against COVID-19 (b). Both vectors are pathological.

a. On the left side is an exemplary graphical output of a vector (in green) in a patient with inflammatory cardiomyopathy. The vector represents the measured area from the beginning of the T-wave until the maximum of T-wave. A wide surface area and vector position in the second quadrant (2) between 90° and 180° are considered pathological.

b. On the right side is an exemplary graphical output of a subject in patients with vaccine-related myocarditis. A broader, larger surface area of the vector is considered pathological.

0.076   0.084